Tailored polyelectrolyte thin film multilayers to modulate cell adhesion

Nicolás E. Muzzio and Miguel A. Pasquale[a)]
Instituto de Investigaciones Fisicoquímicas Teóricas y Aplicadas (INIFTA), (UNLP, CONICET),
Sucursal 4, Casilla de Correo 16, 1900 La Plata, Argentina

Sergio E. Moya[b)]
Soft Matter Nanotechnology group, CIC biomaGUNE, Paseo Miramón 182 C, 20009 San Sebastián,
Gipuzkoa, Spain

Omar Azzaroni[c)]
Instituto de Investigaciones Fisicoquímicas Teóricas y Aplicadas (INIFTA), (UNLP, CONICET),
Sucursal 4, Casilla de Correo 16, 1900 La Plata, Argentina

The layer-by-layer assembly of polyelectrolyte multilayers (PEMs) from natural or synthetic polyelectrolytes constitutes a very versatile and simple strategy to modify surfaces and modulate cell behavior. PEMs assembled from natural polyelectrolytes are very appealing for biological and medical applications due to their high biocompatibility. However, PEMs from natural polyelectrolytes display poor cell adhesion as they are soft materials with an elasticity modulus of a few kilopascal. In this report, the authors present results on the modulation of cell adhesion of different immortalized cell lines by PEMs. Two strategies are employed to vary cell adhesion: (1) a heterogeneous polyelectrolyte multilayer is assembled employing a rigid bottom block including a synthetic polyelectrolyte with a soft upper block of natural polyelectrolytes and (2) polyelectrolyte multilayers from natural polyelectrolytes are thermally annealed after assembly. The physicochemical characteristics of the PEMs change upon thermal treatment. Depending on the composition of the polyelectrolyte multilayer, cell adhesion may be enhanced or reduced. Based on the impact on PEM properties and cell adhesion caused by thermal annealing, a temperature gradient is applied to a PEM of poly-L-lysine/alginate to induce a spatial variation of PEM properties, resulting in a gradient in cell adhesion. The strategies shown here can be employed as simple alternatives to tailor PEM properties by means of fully biocompatible procedures. © 2017 Author(s). *All article content, except where otherwise noted, is licensed under a Creative Commons Attribution (CC BY) license (http://creativecommons.org/licenses/by/4.0/).* [http://dx.doi.org/10.1116/1.5000588]

I. INTRODUCTION

Cell adhesion is the first step of many physiological and pathological cell processes associated with wound healing,[1] bacterial infections,[2] and progression of tumors.[3] Controlling cell adhesion is also a fundamental issue in tissue engineering and medical implants.

Several strategies have been developed to enhance or tune cell adhesion by modifying the chemistry, topography, and mechanical properties of the interface of the substrate interacting with cells, which results in variations in surface energy, wettability, stiffness, and roughness, with a concomitant impact on cell–material interactions.[4–7] Polyelectrolyte multilayer (PEM) films assembled by means of the layer-by-layer (LbL) technique from natural or synthetic polyelectrolytes (PEs) provide a very versatile and simple strategy to modify surfaces and modulate cell functions.[8,9] The LbL technique is based on the alternating assembly of oppositely charged polyelectrolytes, which is mainly driven by electrostatic interactions. The LbL technique has been applied for the engineering of planar substrates or colloidal particles.[10]

The PEM thickness and composition can be controlled with nanometer precision in the vertical direction. In the LbL deposition, besides PEs, other molecules[11,12] such as nanoparticles,[13,14] lipid vesicles,[15] and even cells[16,17] can be assembled on top of multilayers or be placed at selected positions in the PEM, provided that they are charged or exhibit other types of supramolecular interactions with adjacent layers. PEMs fabricated from natural polyelectrolytes, such as poly-L-lysine (PLL), hyaluronic acid (HA), and alginate (Alg), among others, are very appealing for biological and medical applications due to their biocompatibility and biodegradability.[18,19]

In addition, the LbL technique allows for the assembly of growth factors, proteins, peptide sequences, and other biomolecules in the PEM, which can guide and tune cell functions.[4–6] It has been shown that cell adhesion on PEMs can be tuned by changing the conditions for polyelectrolyte assembling, i.e., ionic strength and pH, as well as layer composition. Cell adhesion can also be tuned by increasing the number of deposited layers or by cross-linking them.[8,20–23] Cross-linking has been used for tuning the mechanical properties of PEMs made from biopolymers, as these PEMs usually have a low elastic modulus on the order of few kilopascal[24–26] and cells preferentially adhere to stiffer surfaces. Cross-linking provides stiffness to

[a)]Electronic mail: miguelp@inifta.unlp.edu.ar
[b)]Electronic mail: smoya@cicbiomagune.es
[c)]Electronic mail: azzaroni@inifta.unlp.edu.ar

the PEMs to a degree that correlates with the amount of the cross-linker agent employed, ultimately leading to better cell adhesion. PEM stiffness has also been increased by the assembly of nanoparticles in the PEM structure[9,14] or by capping soft multilayers with a varying number of synthetic polyelectrolyte layers.[21,27] The use of cross-linking agents has the disadvantage that they may not be fully biocompatible. The use of synthetic polyelectrolytes that result in stiffer films in combination with biopolymers has the same drawbacks as the cross-linking since their biocompatibility is limited, discouraging their use for biomedical applications. Moreover, these approaches, especially the cross-linking, may not always result in a large enhancement of cell adhesion, which remains lower than that for uncoated glass surfaces.

Surfaces with gradients in their properties are very appealing for biomedical applications, and a significant amount of research has been invested to obtain a gradual change in the physicochemical properties on the surface of substrates for cell adhesion.[28] PEMs are also more suitable to mimic the extracellular cell matrix by incorporation of gradients in physicochemical properties,[29] which would induce a spatial dependence of cell functionalities and eventually lead to cooperative behaviors. For instance, gradients in PEM *p*H assembly,[30] in PEM stiffness,[29,31] and in the concentration of cell adhesive peptides or growth factors[29,32] have been developed by microfluidic devices, rendering a spatially controlled surface arrangement of biological and physical cues impacting the cellular fate. A spatially controlled swelling ratio in PEMs has been generated by immersing the substrate in a salt gradient.[33] In this work, directional cell migration was observed depending on cell–cell interactions. Furthermore, by time controlled immersion in a solution of natural cross-linkers, a stable stiffness gradient on either free standing PEMs or assembled on silica substrates has been reported, demonstrating differential cell adhesion.[34]

The use of PEMs to modulate cell adhesion requires the development of simple strategies to properly change the physicochemical properties of PEMs of natural polyelectrolytes to tune their behavior toward cell adhesion, either favoring or impeding it, without compromising film biocompatibility. We reported the effect of the proper combination of blocks of polyelectrolytes of different stiffnesses to guide cell adhesion, retaining biocompatibility.[35] Furthermore, we developed a simple procedure to control cell adhesion based on the modification of the physicochemical properties of PEMs by thermal annealing.[36,37] In this report, we show the enhancement of A549 cell adhesion by incorporating a block of rigid PEM made of PLL/poly(sodium 4-styrenesulfonate) (PSS) underneath a PLL/dextran sulfate (Dex) block, as has been demonstrated for the natural PLL/Alg PEM. The effect of thermal annealing on the adhesion properties of PLL/Dex and chitosan (Chi)/HA PEMs is also studied. While cell adhesion is improved for PLL/Dex PEMs, Chi/HA PEMs become antiadhesive for certain cells. Finally, we report results on postassembled PLL/Alg PEMs treated with a temperature gradient between 10 and 50 °C to produce continuous changes in the physicochemical properties that affect cell adhesion. Summing up, the cross-linking free homogeneous or spatially controlled modulation of the physicochemical properties of some natural PEMs toward cell adhesion is described.

II. EXPERIMENT

A. Materials

PLL solution (Mw 70–150 kDa, P4707), PSS (average Mw ∼70 kDa, 243051), poly(allylamine hydrochloride) (PAH, average Mw ∼58 kDa, 283223), poly(diallyldimethyl-lammonium chloride) solution (PDAD, average Mw ∼200–350 kDa, 409022), poly(acrylic acid) solution (PAA, average Mw ∼100 kDa, 523925), Dex sodium salt from *Leuconostoc* spp. (average Mw 9–20 kDa, D6924), sodium chloride, 4-(2-hydroxyethyl)piperazine-1-ethanesulfonic acid sodium salt (HEPES), phosphate-buffered saline (PBS, D1408), bovine serum albumin (BSA), fibronectin (FN) from bovine plasma (F4759), sodium dodecyl sulfate (SDS, L6026), Triton X-100 (T8787), Tween-20 (P9416), thiazolyl blue tetrazolium bromide (MTT, M5655), and dimethyl sulfoxide (DMSO, 472301) were purchased from Sigma-Aldrich. Sodium Alg (Cat. No. 17777-0050), Chi (Mw 100–300 kDa, Cat. No. 349051000), and HA (Mw 1500–2200 kDa, Cat. No. 251770010) were acquired from Acros Organics.

Vinculin, actin cytoskeleton, and cell nucleus were stained using a Focal Adhesion Staining Kit (FAK 100) from Millipore. The Roswell Park Memorial Institute medium (RPMI 1640) with L-glutamine was purchased from Lonza, and fetal bovine serum (FBS) was purchased from Fisher. Nanopure water was obtained using a Barnstead Nanopure Ultrapure Water Purification System.

B. Multilayer film preparation via LbL assembly

All polyelectrolyte solutions were prepared at a concentration of 1 mg ml^{-1} in a 150 mM NaCl, 10 mM HEPES *p*H = 7.4 buffer (HEPES buffer), with the exception of Chi, which was prepared in a 150 mM NaCl, 10 mM sodium acetate buffer (acetate buffer) and adjusted to *p*H 5.0. All solutions were filtered through a 0.45 *μ*m filter. These assembling conditions were selected to ensure PEM stability in physiological conditions.

Cover glasses were cleaned before use as reported previously.[38] Briefly, the glasses were immersed in 10 mM SDS for 3 h, rinsed three times with sterile water, treated with 0.1 M HCl overnight, and thoroughly rinsed with nanopure water. In all PEMs, 15 layers of polyelectrolytes were assembled, with the first and the last layer always being a polycation. Polycations and polyanions were alternately assembled by manual dipping at 24 °C and were allowed to assemble for 15 min. After each layer deposition, films were rinsed three times with water. PEMs were UV-sterilized for 1 h in the laminar flow hood and dried before use.

The LbL assembly for the different polyelectrolyte combinations employed was monitored using a quartz crystal microbalance with a dissipation (QCM-D) Q-Sense E4 system. SiO$_2$ coated quartz crystals (50 MHz, Q-Sense) were

employed. An extended explanation of these experiments was published elsewhere.[35]

To study the effect of thermal annealing on PEMs, samples prepared as described above were left in the incubator at 37 °C for 3 days (annealed PEMs). For some experiments, PEMs were treated with a temperature gradient after assembly. For this purpose, samples were placed on a silver foil of 1 cm wide, 2 cm long, and 0.5 mm thick with one extreme maintained at 10 °C and the other at 50 °C, using thermostated chambers (Fig. 1). The resulting temperature gradient appears to be linear with the distance between sources at fixed temperatures, i.e., 50 and 10 °C.

C. PEM physicochemical characterization

The morphology of air-dried PEMs was studied by atomic force microscopy (AFM) utilizing AFM equipment from Nanowizard II AFM (JPK, Berlin, Germany). Images were collected in the tapping mode using a TESP-V2 cantilever (Bruker, AFM Probes) with a nominal spring constant of 40 N m^{-1} oscillating near a resonant frequency in the range of 280 to 320 kHz. Film elasticity was determined from the nanoindentation experiments performed in buffer solutions in the same AFM equipment.

The wettability of PEMs was evaluated with air-dried samples using a DSA 100 contact angle measuring system (Kruss Company). The tangent angle of a three-phase contact point of a sessile drop profile of nanopure water on PEM surfaces was determined by optical imaging. The volume of the droplet was kept constant (3 μl), while the velocity was set at 500 μl min^{-1}. Four repetitions were conducted for each sample.

The surface charge of the PEM was assessed by measuring the zeta potential on PEM coated colloidal SiO$_2$ particles. For this purpose, SiO$_2$ particles with a diameter of 5 μm were first suspended in HEPES or acetate buffer at 1 mg ml^{-1}. Subsequently, the particles were incubated with the polyelectrolyte solution (1 mg ml^{-1}) for 15 min. The procedure was repeated for every deposited layer up to 15 layers. In between polyelectrolyte depositions, three washing steps were performed via centrifugation. Zeta potential measurements were carried out using a Malvern Zetasizer with a disposable folded capillary cell at 25 °C, applying a cell drive voltage of 40 V and using a monomodal analysis
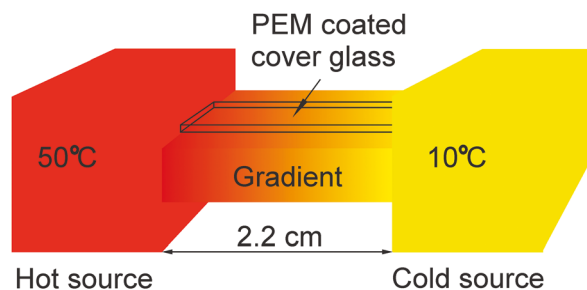
model. Three repetitions were made for each sample. Samples were diluted in either HEPES or acetate buffers at a final concentration of 0.2 mg ml^{-1}. Polyelectrolyte-coated SiO$_2$ particles were annealed following the same protocol as for the annealing of planar films.

The adsorption of BSA and FN proteins on the PEMs before and after annealing was monitored using a QCM-D Q-Sense E4 system. For this purpose, PEMs were assembled on SiO$_2$ coated quartz crystals and immediately placed in the chamber or annealed at 37 °C for three days before use.

D. Cell culture

The A549 epithelial cell line from a human lung carcinoma and C2C12, a mouse myoblast cell line, were grown in the RPMI 1640 medium supplemented with 10% FBS (and antibiotics) and incubated at 37 °C in a 5% CO$_2$ humidified atmosphere. These cell lines were used in various basic studies on polyelectrolyte-coated surfaces.[39–41]

For adhesion assays, glass as control and films on glass supports were placed into petri dishes with a diameter of 35 mm in (Falcon) and UV-sterilized for 1 h,[33] a process widely used and from which no reports indicating significant changes in the PEM properties are known. Then, 5×10^4 cells in 3 ml of culture medium were seeded on top.

E. Quantification of cell adhesion

In order to quantify cell adhesion and cell spreading characteristics, cell contours were manually traced using a Wacom graphic tablet and analyzed using IMAGE-PRO PLUS 6.0 software, Media Cybernetics Inc. The cell area (in μm^2) was determined.[41] Differences in the average cell adhesion area for each PEM and those obtained on glass were evaluated utilizing one-way analysis of variance (ANOVA) and the Fisher test with a significance level of p = 0.05.

F. MTT cell proliferation assay

For MTT experiments, films were assembled in 14 mm circle cover slips and placed in 24-well polystyrene plates. Approximately 2.5×10^4 cells were seeded by adding 1 ml of medium. After 24, 48, and 72 h of incubation, 80 μl of MTT solution (5 mg ml^{-1} in 10 mM PBS) was added into each well. Cells were incubated in the presence of the MTT solution for 3 h at 37 °C. Then, the culture medium was completely removed, and the formazan products were solubilized by adding 600 μl of DMSO to each well. The absorbance spectra were measured at 550 nm using a plate reader (Genios Pro), and the viability was expressed as the number of cells. Measurements were repeated three times, and the mean value and its standard deviation were reported for each condition.

G. Cell immunostaining

Fluorescence staining of vinculin, actin, and cell nucleus was carried out according to the protocol described in the FAK 100 user manual and employing the anti-mouse IgG-

FIG. 1. Scheme of the experimental setup to produce a temperature gradient on the polyelectrolyte multilayer coated glass.

fluorescein isothiocyanate (FITC) conjugated antibody from Millipore as the second antibody. Samples were washed and mounted on a slide by using antifade mounting solution and observed using a confocal laser scanning microscope (Carl-Zeiss LSM 10 META).

III. RESULTS AND DISCUSSION

A. Cell adhesion on natural and synthetic PEMs

The average cell spreading area and the duplication rate of A549 cells for PEMs obtained by assembling natural polycations and polyanions (PLL, Chi, Alg, HA, and Dex) with the synthetic ones (PAH, PDAD, PAA, and PSS) are shown in Figs. 2 and 3. The average cell spreading area is referred to the value obtained from cells on glass, i.e., 870 μm^2. For PEMs assembled with HA, Alg, and Dex irrespective of the polycation except for PDAD, the average cell spreading area was smaller than that obtained by employing PSS as a polyanion for any polycation. For PSS based PEMs, the average cell spreading areas were similar to those obtained from cells adhered to glass. For PDAD, cells exhibited scarce adhesion for all polyanions, mainly due to their toxicity.[42,43] The
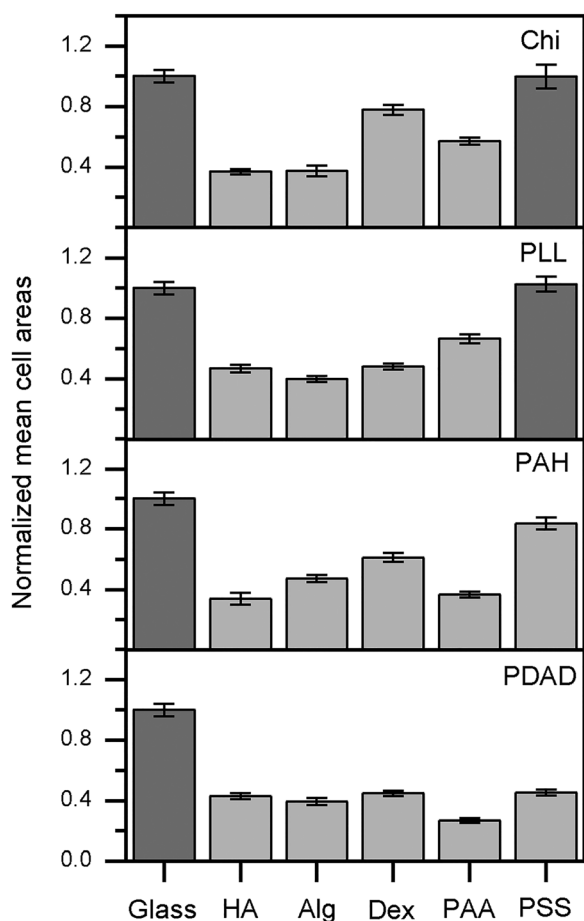
FIG. 2. Normalized A549 cell average adhesion areas for different (polycation/polyanion)$_7$polycation multilayers as indicated. For each PEM, the average cell adhesion areas were smaller than (light gray) or equal to (gray) those on glass employing the ANOVA and Fisher test with 0.05 significance.
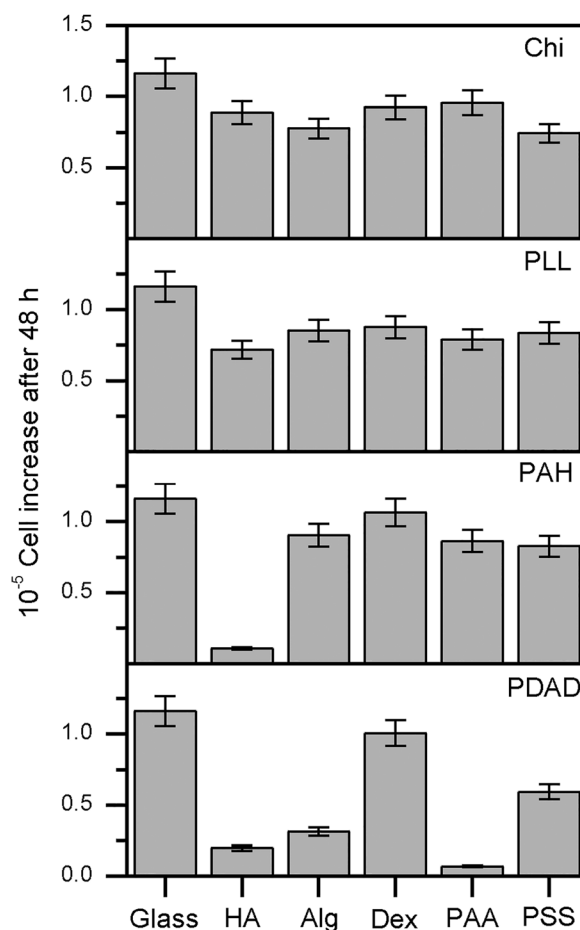
FIG. 3. Cell proliferation expressed as the increase in the number of cells after 48 h of postseeding, for different (polycation/polyanion)$_7$polycation multilayers as indicated.

larger average cell spreading area in PEMs with PSS is consistent with the fact that PSS would increase the rigidity of the PEMs,[44] favoring cell adhesion. For PAA as a polyanion, the average cell spreading area was smaller than with PSS but larger than that obtained from PEMs assembled with any natural polyanion employed here and PLL as a polycation. In general, PAA is a relatively soft material as it retains a large amount of water and is unsuitable for proper cell adhesion. Single cell geometrical characteristics for each PEM were extensively described in previous work.[35]

Cell proliferation was evaluated as the increase in the number of cells after 48 h. Data show that for all PEMs, cell proliferation was smaller than for glass (Fig. 3). The values of cell proliferation relative to those obtained for glass are in the 0.05–0.9 range. The largest cell proliferation was obtained for PEMs assembled with Dex as a polyanion irrespective of the polycation, which is only smaller than that observed for (Chi/PAA)$_7$PAA multilayers. For the latter, although the cell proliferation rate was high, cell adhesion characteristics were poor. The combination of Chi/HA and PLL/Alg resulted in substrates with acceptable cell proliferation, close to 85% of the values observed for glass and exhibiting an exponential increase in the number of cells with time.[35] In general, for PEMs assembled with both

natural polycations and polyanions, the relative proliferation approaches 0.75. PEMs assembled with PSS as a polyanion show a slightly smaller proliferation rate and a linear increase in the number of cells with time.[35]

To summarize, the combination of biological polyelectrolytes resulted in poorer cell adhesion than the one observed for glass or for many synthetic polyelectrolyte multilayers, especially that for PEMs with PSS. Furthermore, the PEM composition affects cell adhesion and proliferation differently. Particularly, for PEMs with PSS and good cell adhesion, proliferation is poorer than that for glass.

B. Simple strategies to modify PEM cell adhesion characteristics

In the Subsecs. III B 1–III B 3, two simple strategies to modify cell adhesion on PEMs made of natural or biological polyelectrolyte thin films are presented.

1. Heterogeneous PEMs to improve cell adhesion

With the aim of increasing the cell adhesion properties of natural biocompatible films, two blocks of PEMs with two different polyelectrolyte combinations were subsequently assembled. The first block was formed with PSS and PLL to reinforce the PEM mechanical properties and to increase cell adhesion on the resulting system. The top PEM layers were always composed of a biopolymer combination displaying moderate cell adhesion but an acceptable cell proliferation rate, $(PLL/Alg)_nPLL$ and $(PLL/Dex)_nPLL$.

The best adhesion properties were obtained for top blocks formed by two bilayers, n = 2, while for n > 4, i.e., top PEMs with more than two bilayers, cell adhesion was rather poor. Heterogeneous PEMs appeared to have different properties toward cell adhesion than those observed on each single block PEM. In fact, the physicochemical properties are different between PEMs assembled upon a pair of polyelectrolytes (homogeneous) and heterogeneous PEMs. QCM-D data show that the assembly of PLL/PSS is rather supralinear at least for 12 layers, and then, the growth of the subsequent $(PLL/Alg)_nPLL$ multilayer follows a linear trend.[35] In contrast, the assembly of PLL/Alg PEM from a glass substrate displays supralinear growth. Furthermore, atomic force microscopy images show a smoother topography for PLL/Alg assembled on top of the PLL/PSS underneath the block than that assembled on glass.[35]

The $(PLL/PSS)_6(PLL/Dex)_nPLL$ heterogeneous PEMs exhibit the same behavior that has been reported for $(PLL/PSS)_6(PLL/Alg)_nPLL$.[35] The results from cell adhesion experiments employing both $(PLL/PSS)_6(PLL/Dex)_nPLL$ and $(PLL/PSS)_6(PLL/Alg)_nPLL$ are shown in Fig. 4. The cell cytoplasm and nucleus fluorescence staining allow a better appreciation of the differences in adhesion properties between the single block and diblock PEMs. Tetramethylrhodamine (TRITC)-conjugated phalloidin staining of cells adhered to $(PLL/PSS)_6(PLL/Dex)_nPLL$ or $(PLL/PSS)_6(PLL/Alg)_nPLL$ heterogeneous multilayers allows the visualization of long actin fibers needed for

cytoplasm spreading and focal contact formation. In this case, a large number of well-developed focal contacts can be distinguished in cells adhered to diblock PEMs in comparison with $(PLL/Alg)_7PLL$ or $(PLL/Dex)_7PLL$ multilayers.

The results described above can be interpreted as a consequence of polyelectrolyte interdigitation during or after assembling. Layer interdigitation generates PEMs with physicochemical properties that are absent on each block system. PSS molecules from the inner block are likely to be present in the outer block, and polycation molecules are expected to move through each block. It is widely accepted that interdigitation processes occur in PEMs.[45–48] When a polyelectrolyte layer is assembled in a PEM, it can affect the film up to four neighbor layers.

2. Cell adhesion enhancement by thermal annealing of PEMs

The thermal treatment at 37 °C for three days modifies the physicochemical properties of PEMs, inducing changes in cell adhesion properties. Previous data showed that similar results were obtained at a higher temperature and for a shorter time of annealing. The treatment at 37 °C for 3 days ensures stable changes in all samples tested. Cell adhesion properties improve in annealed PLL/Alg and PLL/Dex films.

The changes in the physicochemical properties of PEMs upon annealing at different temperatures have been extensively described in previous publications.[36,37] In these papers, the topography of PEMs after annealing was assessed by AFM on air-dried PEMs. Film elasticity upon annealing was determined from the nanoindentation experiments performed in HEPES buffer using the same AFM equipment acquiring force–distance curves. AFM characterization suggested that upon annealing, the film becomes smoother and stiffer [Figs. 5(a)–5(d)], with the average roughness changing from close to 4.3 nm to about 2.3 nm.

The zeta potential was measured on PEM coated colloids diluted in 10 mM HEPES, 150 mM NaCl (pH 7.4) buffer at a final concentration of 0.1 mg ml^{-1}. Although the differences in the procedure to obtain colloidal PEMs in comparison with the linear ones may produce changes in the coating properties, the change in zeta potential between nonannealed and annealed PEMs allows inferring the evolution of the charge in PEMs upon annealing. The zeta potential changes from about zero before annealing to ca. -14 mV after annealing, meaning that the density of charged groups on the PEM surface has increased after annealing. Changes in PEM wettability were determined on air-dried samples by measuring the contact angle of constant volume liquid drops. The contact angle [Figs. 5(e) and 5(f)] increases from $36° \pm 3°$ to $92° \pm 4°$ and concomitantly, its surface energy, indicating an augmented hydrophobic character.[37]

BSA and FN were used as model proteins to characterize protein adsorption on samples in order to get more information about the impact of the annealing process on the behavior of the film with the cell in the culture medium, where BSA is the most abundant protein and FN is a typical protein
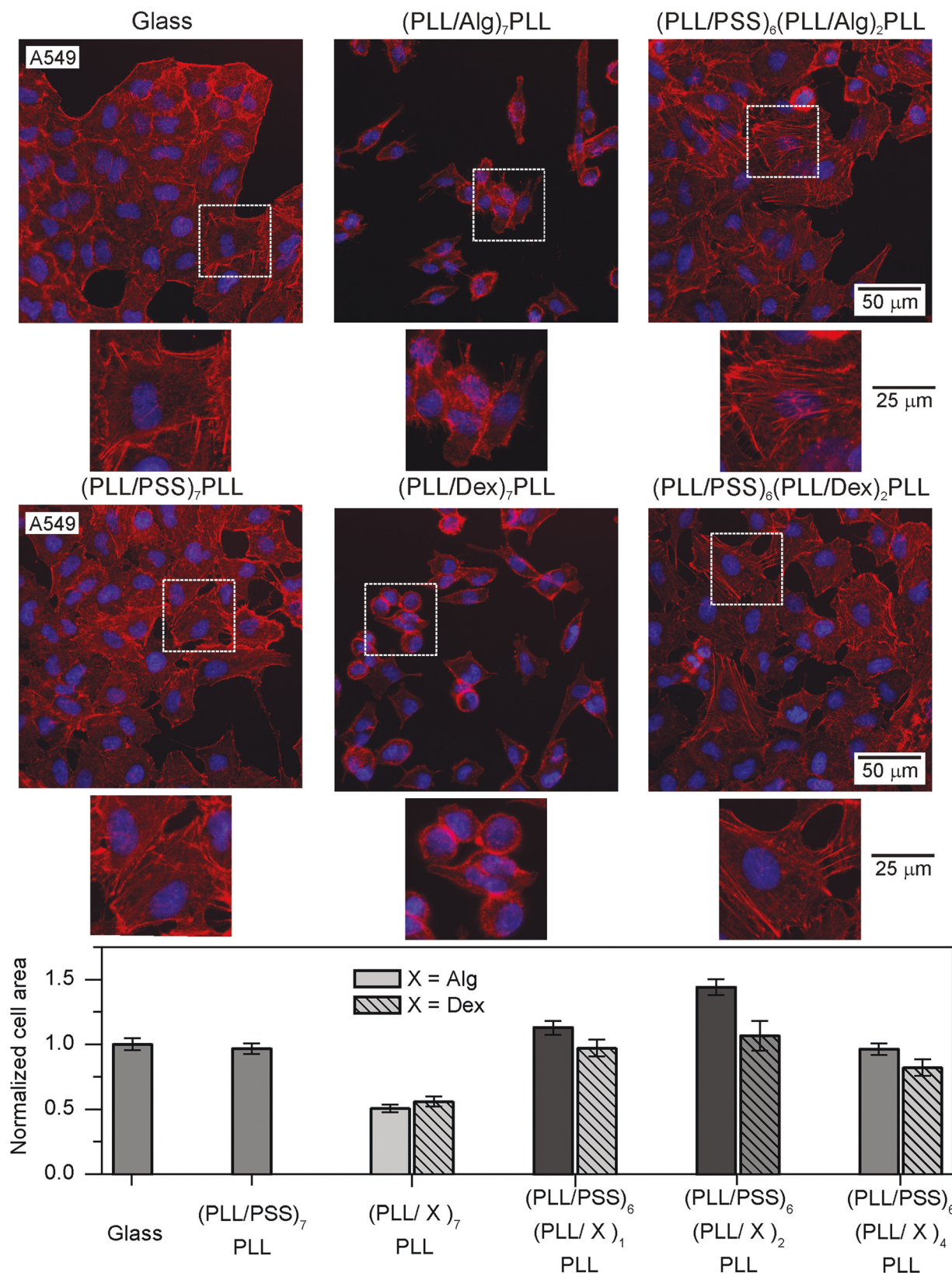
FIG. 4. Heterogeneous PEM assembly to improve A549 cell adhesion properties. Confocal laser scanning microscopy images of TRITC-conjugated phalloidin and DAPI stained cells on glass and homogeneous and heterogeneous PEMs, as indicated. Enlarged images of the areas indicated by squares are included to better appreciate actin filaments. The best results are obtained for $(PLL/PSS)_6 (PLL/Alg)_2PLL$ and $(PLL/PSS)_6(PLL/Dex)_2PLL$ multilayers, as is shown by the relative average cell spreading area for the different systems (bar graphs in the figure). In the case of $(PLL/PSS)_6(PLL/Alg)_2$ multilayers, the relative average spreading area is larger than that observed on glass or on $(PLL/PSS)_6PLL$ multilayers. For each PEM, the average cell adhesion areas were smaller than (light gray), equal to (gray), or larger than (dark gray) that on glass employing the ANOVA and Fisher test with 0.05 significance.
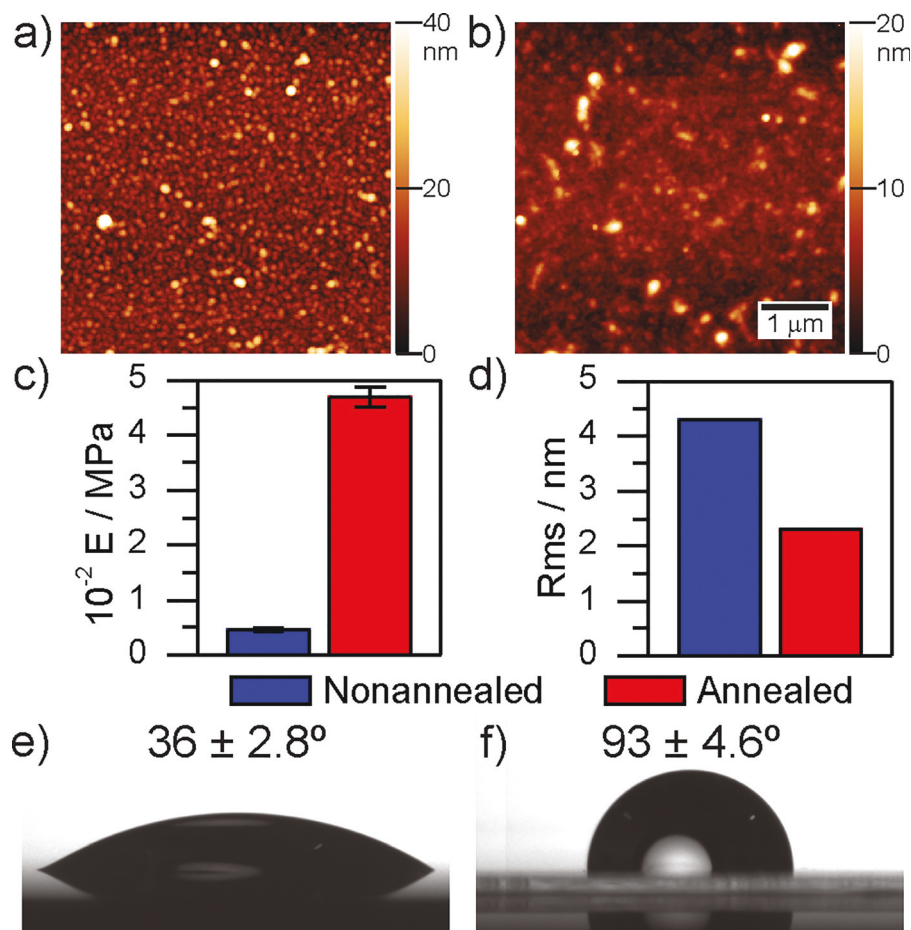
FIG. 5. Physicochemical properties and cell adhesion characteristics of nonannealed and annealed (PLL/Alg)$_7$PLL multilayers. AFM images of nonannealed (a) and annealed (b) (PLL/Alg)$_7$PLL multilayers. The Young's modulus, E, (c) and the roughness (d) of nonannealed and annealed PEMs are depicted in bar graphs. Changes in the contact angle of nonannealed and annealed PEMs averaged from four experiments are shown [(e) and (f), respectively].

that promotes cell adhesion. PEMs are charged, and as such, they can interact with proteins, which will deposit on the film due to electrostatic interactions. The results from QCM-D experiments showed that BSA protein adsorption decreased in annealed samples, as deduced from an approximately fourfold decrease in the value of −ΔF after the adsorption of proteins on annealed samples in QCM-D measurements [Figs. 6(a) and 6(b)]. On the other hand, FN adsorption exhibited the reverse behavior. Upon annealing, PLL/Alg PEMs showed a larger value of −ΔF when FN solution was passed through the chamber in comparison with nonannealed PEMs [Figs. 6(c) and 6(d)]. Upon annealing, PLL/Alg PEM adsorbed a larger amount of FN, a protein that mediates cell adhesion. It should be pointed out that FN in an amount as low as $20 \, \mathrm{ng \, cm^{-2}}$ (about 5 Hz) is expected to promote cell adhesion.[49] Furthermore, not only protein surface concentration but also protein conformation are relevant parameters for cell adhesion.[50] Summing up, the changes in the film properties described above would interplay in a complex manner, producing the change of PLL/Alg PEMs from antiadhesive to adhesive after annealing [Figs. 6(e) and 6(f)].

The above data indicate that the thermal annealing of (PLL/Alg)$_7$PLL multilayers induces the reorganization of

polyelectrolyte chains,[37] and as a consequence of the differences in the molar weight between the polyanion and the polycation, the negative charge at the surface increases. Polyelectrolyte multilayers of poly(diallyl dimethyl ammonium chloride) and poly(styrene sodium sulfonate) in the form of capsules show a structural rearrangement after annealing.[51–53] This fact has been interpreted by a maximization of the polyelectrolyte electrostatic interaction enhanced by the increase in polyelectrolyte motility inside the multilayer. Recent studies related to the effect of thermal treatment on the internal structure of PEMs have been conducted using the neutron reflectometry technique.[54] For the PEMs before and after annealing, no changes in the X-ray photoelectron spectroscopy spectra with respect to the binding energies associated with N–CO/C–NH$_2$ and C–NH$_3$ bonds and the molar percentages of C, O, and N could be observed between the reference spectra of nonannealed PEMs and PEMs annealed at 37 °C.[37] Therefore, it can be concluded that the annealing does not alter the chemistry of the multilayers but leads only to a reorganization of the film.

Another PEM combination can lead to an increase in cell adhesion after annealing. Indeed, (PLL/Dex)$_7$PLL multilayers become adhesive for A549 cells after annealing (Fig. 7),
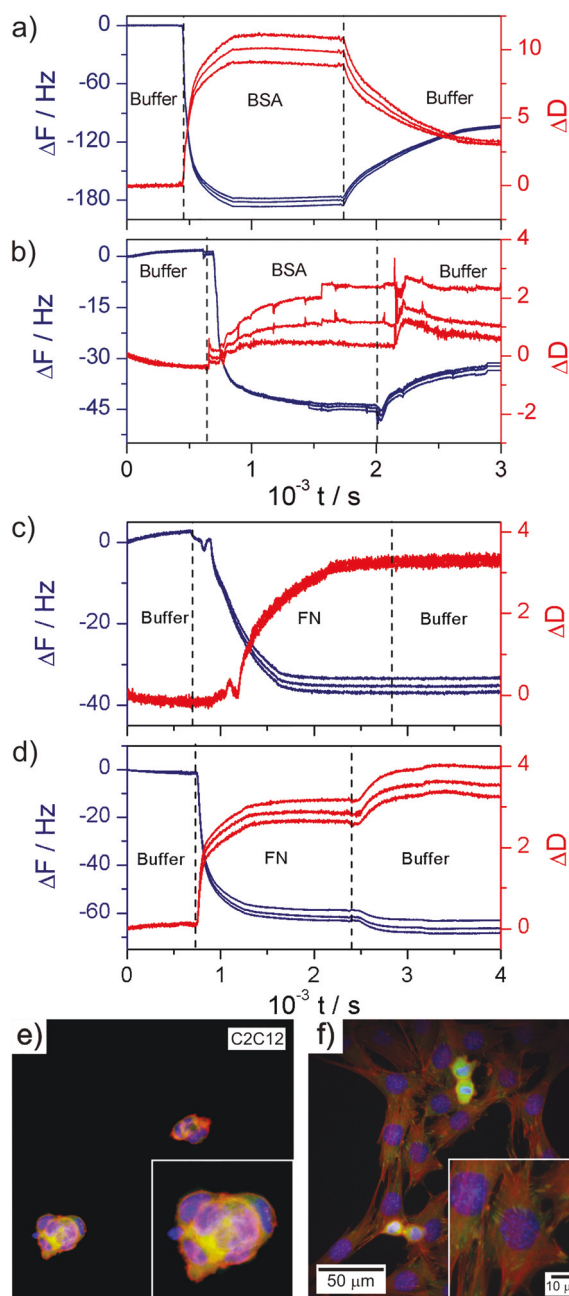
FIG. 6. QCM-D data for the third, fifth, and seventh harmonics from BSA adsorption on nonannealed (PLL/Alg)₇PLL multilayer (a) and annealed (PLL/Alg)₇PLL multilayer (b). QCM-D data from FN adsorption on nonannealed (PLL/Alg)₇PLL multilayer (c) and annealed (PLL/Alg)₇PLL multilayer (d). Dashed lines indicate the change from pure buffer to protein solution and vice versa. Immunostaining of vinculin (green) and staining of actin (red) and cell nucleus (blue) of C2C12 myoblast cells on (PLL/Alg)₇PLL before and after annealing [(e) and (f), respectively]. Enlarged images are shown in the inset.

similar to the behavior reported for (PLL/Alg)₇PLL multilayers. For both PEMs, the average cell spreading area relative to that obtained on glass was 0.55 before annealing. After annealing, the cell spreading area reached a similar value to that obtained for glass, i.e., $870\ \mu m^2$. The actin fibers stained with TRITC-conjugated phalloidin are longer in cells adhered to annealed PEMs than to the nonannealed

ones. These fibers, more clearly appreciated at the cell edges, define the extension of the cytoplasm and focal contact formation.

3. Enhancement of the antiadhesive properties of thermally annealed Chi/HA PEM

In contrast to the cell adhesion enhancement reported above for PLL/Alg and PLL/Dex PEMs, (Chi/HA)₇Chi
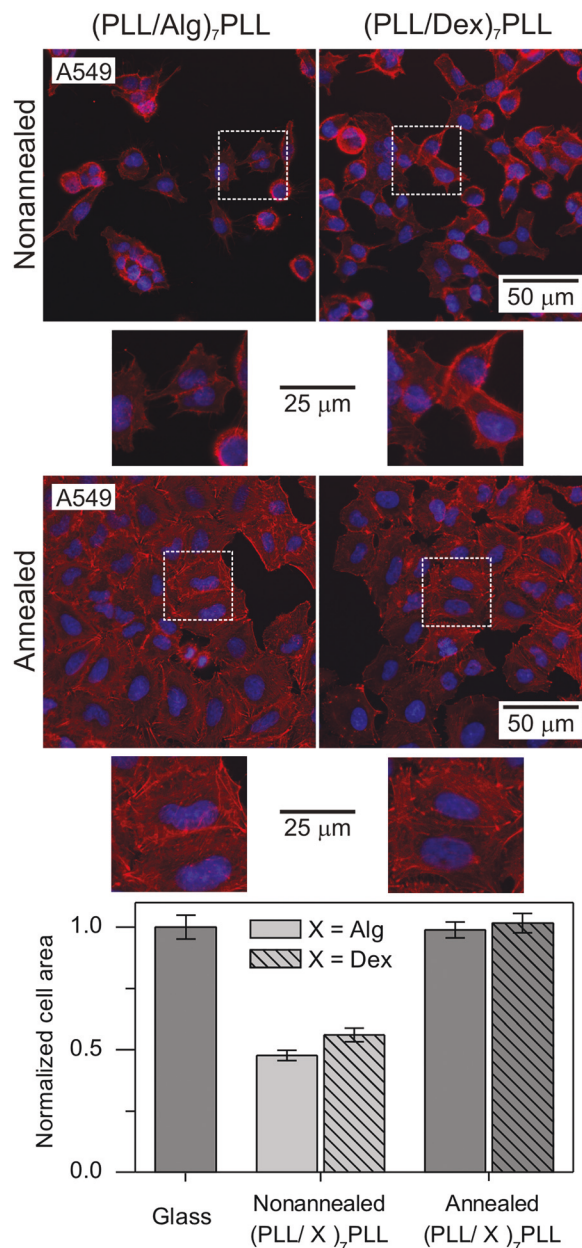

FIG. 7. Cell adhesion enhancement after annealing at 37 °C. Confocal epifluorescence microscopy images of cytoplasm and nucleus stained A549 cells cultured on nonannealed and annealed PEMs. Enlarged images of the areas indicated by squares are included to better appreciate actin filaments. The average relative cell spreading area on (PLL/Alg)₇PLL and (PLL/Dex)₇PLL becomes similar to that observed on glass upon annealing. The standard errors are included in the bar graphs. The grayscale colors indicate significant differences between average cell spreading areas of cells in the different samples (p = 0.05).

multilayers annealed at 37 °C for three days generate an enhanced antiadhesive surface, in contrast to the behavior observed.

The effect of annealing at 37 °C on some physicochemical properties of PEMs assembled with Chi as a polycation and HA as a polyanion was measured (Fig. 8).

AFM measurements of Chi/HA PEMs after being immersed in HEPES buffer and dried [Figs. 8(a) and 8(b)] revealed that the surface becomes smoother at the submicrometer scale with the annealing, as in the case of PLL/Alg PEMs, but while for the latter, a granular homogeneous structure is formed, for Chi/HA PEMs, a fibrillar network can be distinguished. The thermal annealing causes the fibers to become thinner and more bidimensional, i.e., the surface

is covered with structures having an average height close to 5 nm, a value significantly smaller than those measured for the nonannealed PEM. The elasticity of Chi/HA PEMs was determined from nanoindentation experiments [Fig. 8(d)]. In contrast to the changes in the Young's modulus observed for PLL/Alg multilayers, no conclusive Young's modulus differences between nonannealed and annealed Chi/HA PEMs could be determined.

Contact angle values were determined on nonannealed and annealed Chi/HA PEMs [Fig. 8(f)]. The former exhibited a contact angle of $30.2° \pm 0.3°$, and after annealing, the contact angle decreased to values of $20.6° \pm 1.8°$. From these data, we can conclude that although the nonannealed PEMs are hydrophilic, the thermal annealing increases the
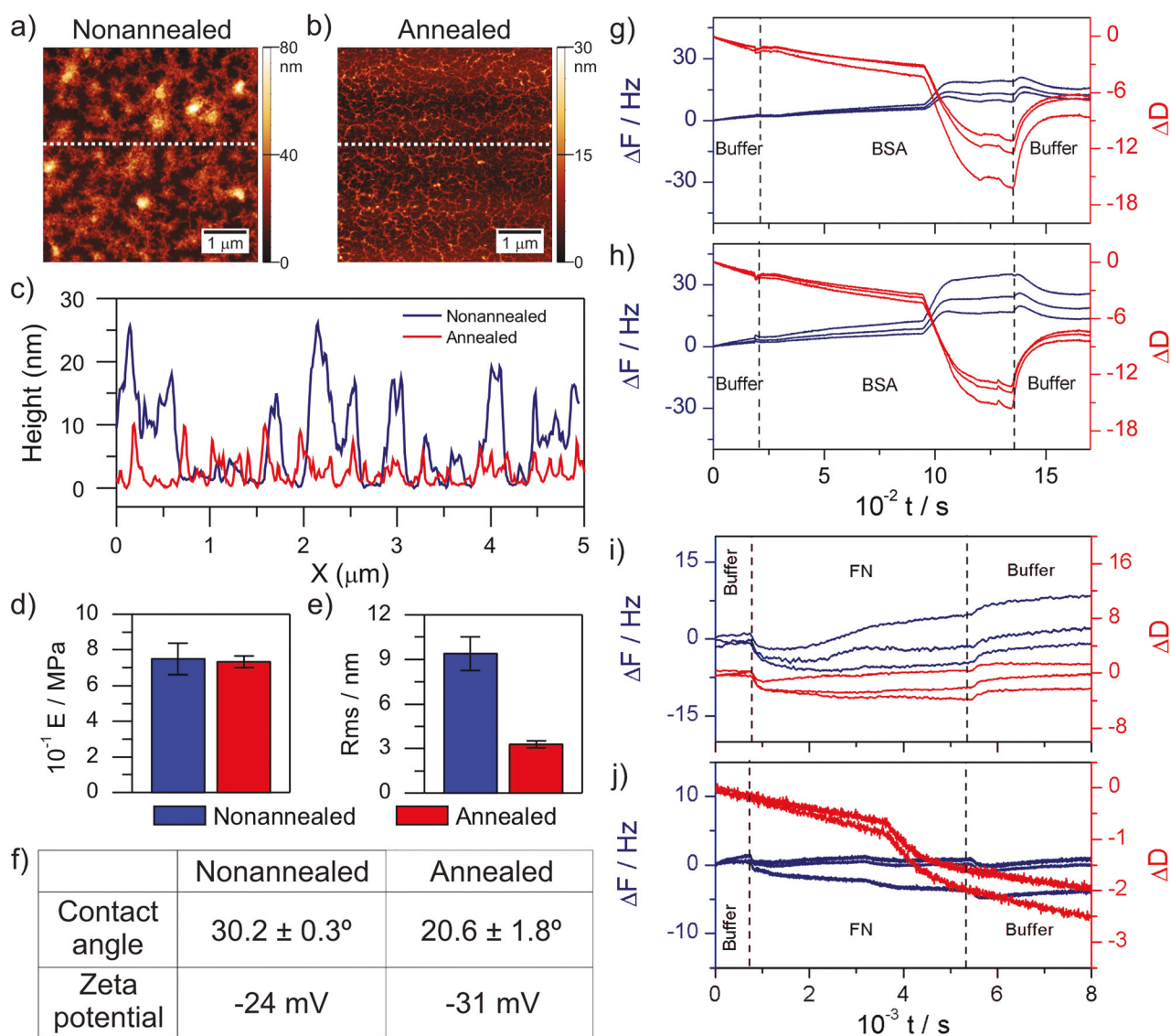

FIG. 8. Physicochemical properties and cell adhesion characteristics of nonannealed and annealed (Chi/HA)$_7$Chi multilayers. AFM images of nonannealed (a) and annealed (b) (Chi/HA)$_7$Chi multilayers. AFM line profile from images depicted in (a) and (b) as indicated by the discontinuous line (c). The Young's modulus (d) and the roughness (e) of nonannealed and annealed PEMs are depicted in bar graphs. Average contact angle and zeta potential data for nonannealed and annealed PEMs are shown (f). QCM-D data for the third, fifth, and seventh harmonics from BSA adsorption [(g) and (h)] on nonannealed (Chi/HA)$_7$Chi multilayer (g) and annealed (Chi/HA)$_7$Chi multilayer (h). QCM-D data from FN adsorption on nonannealed (Chi/HA)$_7$Chi multilayer (i) and annealed (Chi/HA)$_7$Chi multilayer (j). Dashed lines in (g)–(j) indicate the time at which HEPES buffer or protein solution is flown through the QCM cell.

hydrophilic character of the PEMs. The zeta potential measurements of Chi/HA PEMs in HEPES buffer indicate a negative charge on the surface of these films for both the nonannealed and annealed PEMs, being -24 mV for the former and -31 mV for the latter. QCM-D data [Fig. 8(g)–8(j)] exhibit a rather complex behavior and suggest that neither BSA nor FN protein adsorption can feasibly be detected by this technique. Thus, either nonannealed or annealed Chi/Ha PEMs result in antifouling substrates.

The observed adhesion properties were cell-type dependent. For C2C12 cells, the average cell spreading area diminishes to about a half of that measured before annealing; for the latter, it was close to that found on glass ($920 \, \mu m^2$). For A549 cells, the adhesion was poor either before or after annealing (Fig. 9).

The changes in the physicochemical properties of Chi/HA PEMs indicate an increase in the hydrophilicity and the negative charge and a decrease in the roughness of PEM upon annealing. Furthermore, no differences in stiffness and protein adsorption between annealed and nonannealed PEMs were detected. The magnitude of the changes in the contact angle and surface charge is rather small to take account for the changes in cell adhesion properties, and thus, changes in Chi/HA film topography upon annealing would play a key role. It has been extensively reported that the topographic characteristics of the substrate at different size scales have a great influence on cell functionality.[55,56] In general, cells tend to adhere to rougher surfaces displaying features at the micro- and nanoscale. Annealed Chi/HA PEMs show less roughness, are more planar, and cover the substrate more homogenously. These facts are coherent with a lower cell adhesion.

The above data from adhesive and antiadhesive films show that thermal annealing changes the physicochemical properties of each PEM tested differently and modulates cell adhesion in a cell-dependent manner. PEM stiffness has been reported to play a key role in cell adhesion,[14,20,41] but it should be pointed out that other factors impact cell adhesion. Moreover, PEMs tested in this report are a few tens of nanometers, and it is known that cells are able to sense the rigidity of the underneath glass substrate, even several polymer layers below.[21] Possibly, the changes in physicochemical properties would affect the adsorption of different types of proteins and the degree of coverage, and even more importantly, protein conformation play a role in driving cell adhesion and spreading, as reported.[57,58]

C. Thermal gradient to locally modulate PEM adhesion properties

Employing the experimental setup described above (Fig. 1), a temperature variation between 50 and 10 °C was applied along the whole length of a glass substrate coated with the (PLL/Alg)$_7$PLL multilayer. The resulting temperature gradient was close to $0.002 \, °C \, \mu m^{-1}$.

A continuous change in the physicochemical properties appears to set in along the substrate upon the application of a
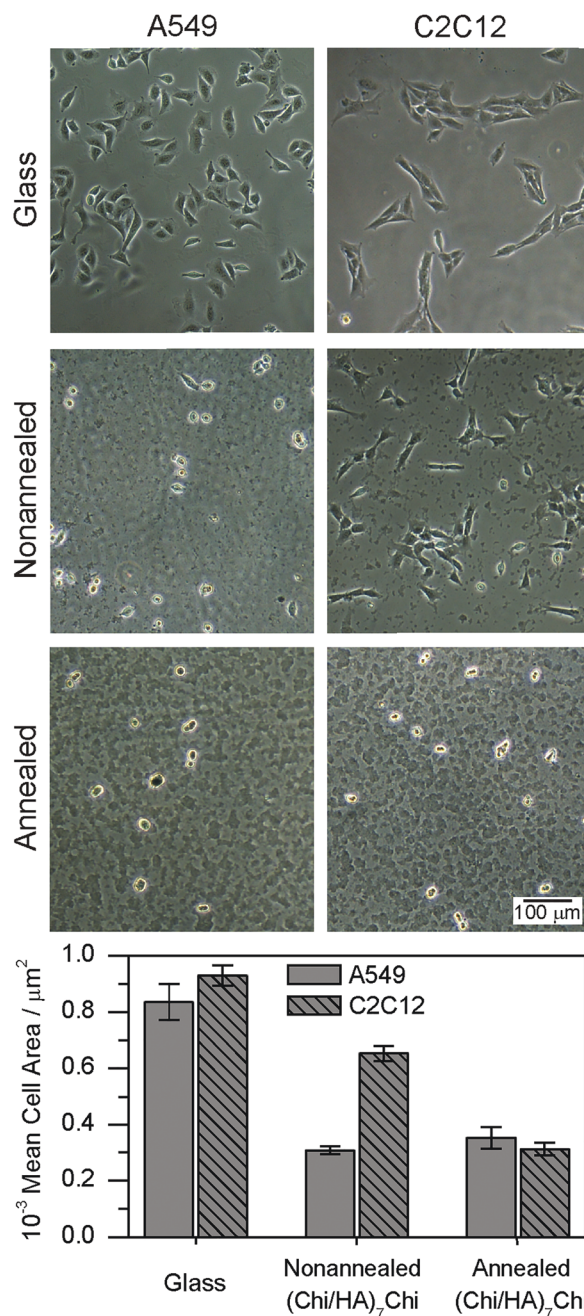

FIG. 9. Cell adhesion characteristics of nonannealed and annealed (Chi/HA)$_7$Chi multilayers for A549 and C2C12 cell lines. For A549 cells, no significant effect is observed upon annealing, but for C2C12 myoblast, a clear decrease in cell adhesion is measured.

thermal gradient (Fig. 10). The observed values of contact angles along the gradient are close to those observed in PEMs annealed at a uniform temperature. Moreover, the adsorption of FITC-labeled BSA protein decreased in going from the side at the lowest temperature to the side at the highest temperature.

For the substrate region held at the highest temperature, C2C12 cell adhesion was roughly close to that observed on glass. In contrast, in the coldest region, cell adhesion was very poor. More significant changes in the average cell spreading area were observed between T2 = 30 and T1 = 22 °C, as shown
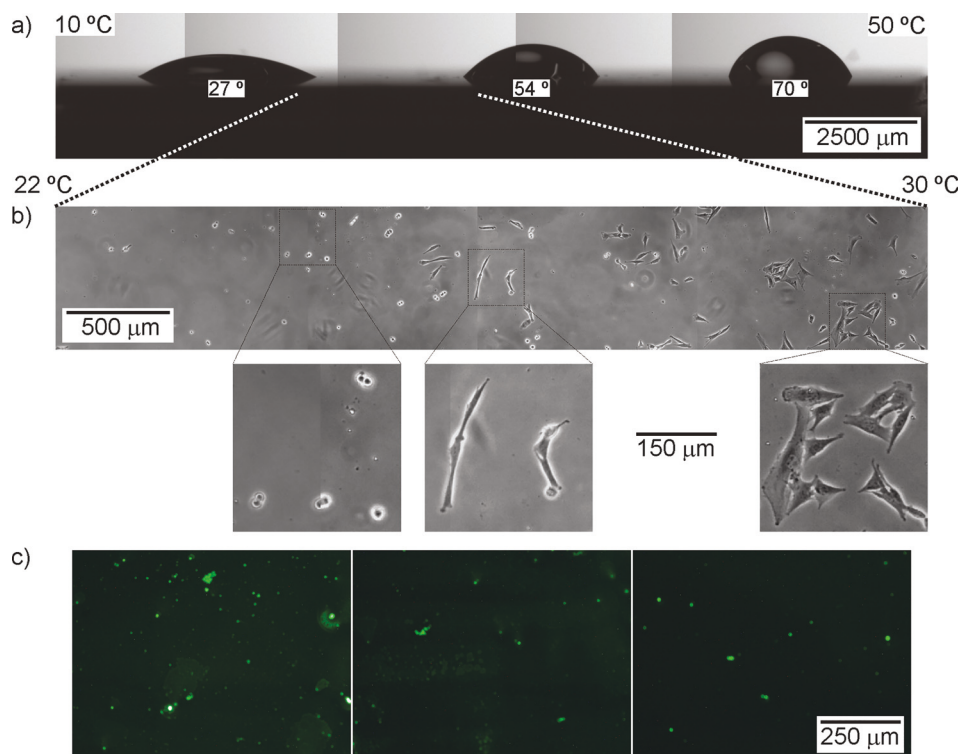
FIG. 10. Effect of a thermal gradient on the surface wettability, cell adhesion characteristics, and adsorption of labeled BSA protein. Contact angle measured at PLL/Alg PEM sites annealed at different average temperatures (a). Phase contrast images of C2C12 myoblast cells adhered to PEM regions thermally treated between 22 and 30 °C (b). The changes in the PEM physicochemical properties induced along the 22–30 °C temperature gradient produce significant changes in cell adhesion properties, as indicated by dashed lines in (a) and (b). The minimum and maximum temperatures for all regions are included. Enlarged images of regions indicated by dashed squares are shown to better appreciate the changes in the cell morphology along the film after the treatment with the temperature gradient. FITC-labeled BSA adsorbed on three different regions of PLL/Alg PEM thermally treated (c). The fluorescence intensity is higher for the region at lower temperature.

in Fig. 10. The average cell spreading area at $T2 - \Delta T$ was $260 \pm 15 \, \mu m^2$, and at $T1 + \Delta T$, it was $715 \pm 20 \, \mu m^2$, with $\Delta T = 3 \, °C$.

It is worth noting that upon thermal annealing, PEMs exhibit a continuous change in their wettability although cell adhesion changes significantly in a narrower temperature range. The clearest effect on the average cell spreading area appears to be between 22 and 30 °C. This is in consonance with the fact that in the case of uniform thermal annealing of samples, 37 °C is enough to induce significant changes in cell adhesion properties.

The application of a thermal gradient to locally modify the physicochemical properties of films as well as the adhesion characteristics toward different cell lines can be extended to other polymeric systems to increase the versatility of new materials for rapid testing of cell functionalities.

IV. SUMMARY AND CONCLUSIONS

In this report, two simple strategies to modulate cell adherence to PEMs made of natural polyelectrolytes are presented. For (PLL/Dex) PEMs, cell adhesion is enhanced by assembling a $(PLL/Dex)_n$ block on top on an inner block of the $(PLL/PSS)_6$ film or by thermal annealing at 37 °C. On the other hand, for Chi/HA PEMs, thermal annealing enhances antiadhesive properties in a cell type-dependent manner.

We show results on cell adhesion on PEMs assembled by the combination of both natural and synthetic polyelectrolytes. In general, PEMs with both natural polycations and polyanions result in surfaces with poor cell adhesion. In contrast, PLL/PSS based PEMs exhibit improved adhesion, at least for the tested cell lines. Thus, a heterogeneous construction employing $(PLL/PSS)_6$ as an inner block and $(PLL/Alg)nPLL$ or $(PLL/Dex)nPLL$ as an upper block is proposed to improve cell adhesion without losing biocompatibility. The best results were obtained for $n = 2$. The results are explained by interdigitation of polyelectrolytes.

The other strategy to modulate cell adhesion is the thermal annealing of PEMs. $(PLL/Alg)_7PLL$ and $(PLL/Dex)_7PLL$ multilayers improve cell adhesion properties upon thermal annealing. In contrast, $(Chi/HA)_7Chi$ multilayers show a decrease in the average cell spreading area after annealing. The thermal energy would increase the polyelectrolyte chain mobility and favor a maximization of the interactions between polyelectrolytes, resulting in an increase in the contact angle and a decrease in surface charge. This is reflected in changes in the adsorption of proteins and in cell adhesion, concomitantly with the cell phenotype.

Finally, based on the results from thermal annealing at uniform temperature, a thermal gradient with temperatures in the 10−50 °C range was applied to PLL/Alg PEMs with the aim of producing a continuous change in the physicochemical

properties that affect cell adhesion. Surfaces with gradients of properties are important to produce materials that better mimic the extracellular matrix interacting with cells and are of particular interest for basic studies of the interactions between biological species and surfaces since the gradual impact of a selected property can be examined in a single experiment.

ACKNOWLEDGMENTS

[1]E. Lih, S. H. Oh, Y. K. Joung, J. H. Lee, and D. K. Han, Prog. Polym. Sci. **44**, 28 (2015).

[2]N. Saha, C. Monge, V. Dulong, C. Picart, and K. Glinel, Biomacromolecules **14**, 520 (2013).

[3]E. di Martino, G. Kelly, J.-A. Roulson, and M. A. Knowles, Mol. Cancer Res. **13**, 138 (2015).

[4]T. Boudou, T. Crouzier, K. Ren, G. Blin, and C. Picart, Adv. Mater. **22**, 441 (2010).

[5]J. Borges and J. F. Mano, Chem. Rev. **114**, 8883 (2014).

[6]C. Monge, J. Almodóvar, T. Boudou, and C. Picart, Adv. Healthcare Mater. **4**, 811 (2015).

[7]M. P. Sousa, S. G. Caridade, and J. F. Mano, Adv. Healthcare Mater. **6**, 1601462 (2017).

[8]R. R. Costa and J. F. Mano, Chem. Soc. Rev. **43**, 3453 (2014).

[9]V. Gribova, R. Auzely-Velty, and C. Picart, Chem. Mater. **24**, 854 (2012).

[10]J. Zhou, G. Romero, E. Rojas, L. Ma, S. Moya, and C. Gao, J. Colloid Interface Sci. **345**, 241 (2010).

[11]V. Fitzpatrick, L. Fourel, O. Destaing, F. Gilde, C. Albigès-rizo, C. Picart, and T. Boudou, Sci. Rep. **7**, 41479 (2017).

[12]M. Kumorek, O. Janoušková, A. Höcherl, M. Houska, E. Mázl-chánová, N. Kasoju, L. Cuchalová, R. Matějka, and D. Kubies, Appl. Surf. Sci. **411**, 240 (2017).

[13]T. Kruk, K. Szczepanowicz, D. Kręgiel, L. S. Warszyńska, and P. Warszyński, Colloids Surf. B **137**, 158 (2016).

[14]S. Schmidt, N. Madaboosi, K. Uhlig, D. Köhler, A. Skirtach, C. Duschl, H. Möhwald, and D. V. Volodkin, Langmuir **28**, 7249 (2012).

[15]D. Volodkin, A. Skirtach, and H. Möhwald, Adv. Polym. Sci. **240**, 135 (2010).

[16]J. M. Mets, J. T. Wilson, W. Cui, and E. L. Chaikof, Adv. Healthcare Mater. **2**, 266 (2013).

[17]A. Nishiguchi, H. Yoshida, M. Matsusaki, and M. Akashi, Adv. Mater. **23**, 3506 (2011).

[18]T. Crouzier, T. Boudou, and C. Picart, Curr. Opin. Colloid Interface Sci. **15**, 417 (2010).

[19]J. M. Silva, R. L. Reis, and J. F. Mano, Small **12**, 4308 (2016).

[20]H. Chang, H. Zhang, M. Hu, X. Chen, K. Ren, J. Wang, and J. Ji, Biomater. Sci. **3**, 352 (2015).

[21]L. Kocgozlu, P. Lavalle, G. Koenig, B. Senger, Y. Haikel, P. Schaaf, J.-C. Voegel, H. Tenenbaum, and D. Vautier, J. Cell Sci. **123**, 29 (2010).

[22]C. Chaubaroux *et al.*, Biomacromolecules **13**, 2128 (2012).

[23]J. M. Silva, J. R. García, R. L. Reis, A. J. García, and J. F. Mano, Acta Biomater. **51**, 279 (2017).

[24]C. Picart, B. Senger, K. Sengupta, F. Dubreuil, and A. Fery, Colloids Surf. A **303**, 30 (2007).

[25]A. J. Engler, L. Richert, J. Y. Wong, C. Picart, and D. E. Discher, Surf. Sci. **570**, 142 (2004).

[26]A. Schneider *et al.*, Langmuir **22**, 1193 (2006).

[27]G. Francius, J. Hemmerlé, V. Ball, P. Lavalle, C. Picart, J.-C. Voegel, P. Schaaf, and B. Senger, J. Phys. Chem. C **111**, 8299 (2007).

[28]M. S. Kim, G. Khang, and H. B. Lee, Prog. Polym. Sci. **33**, 138 (2008).

[29]J. Almodóvar, T. Crouzier, Š. Selimović, T. Boudou, A. Khademhosseini, and C. Picart, Lab Chip **13**, 1562 (2013).

[30]K. Kirchhof, A. Andar, H. B. Yin, N. Gadegaard, M. O. Riehle, and T. Groth, Lab Chip **11**, 3326 (2011).

[31]J. S. Martinez, A. M. Lehaf, J. B. Schlenoff, and T. C. S. Keller, Biomacromolecules **14**, 1311 (2013).

[32]J. Almodóvar, R. Guillot, C. Monge, J. Vollaire, Š. Selimović, J.-L. Coll, A. Khademhosseini, and C. Picart, Biomaterials **35**, 3975 (2014).

[33]L. Han, Z. Mao, J. Wu, Y. Guo, T. Ren, and C. Gao, Biomaterials **34**, 975 (2013).

[34]J. M. Silva, S. G. Caridade, N. M. Oliveira, R. L. Reis, and J. F. Mano, J. Mater. Chem. B **3**, 4555 (2015).

[35]N. E. Muzzio, M. A. Pasquale, D. Gregurec, E. Diamanti, M. Kosutic, O. Azzaroni, and S. E. Moya, Macromol. Biosci. **16**, 482 (2016).

[36]N. E. Muzzio, D. Gregurec, E. Diamanti, J. Irigoyen, M. A. Pasquale, O. Azzaroni, and S. E. Moya, Adv. Mater. Interfaces **4**, 1600126 (2017).

[37]E. Diamanti, N. Muzzio, D. Gregurec, J. Irigoyen, M. Pasquale, O. Azzaroni, M. Brinkmann, and S. E. Moya, Colloids Surf., B **145**, 328 (2016).

[38]A. L. Hillberg, C. A. Holmes, and M. Tabrizian, Biomaterials **30**, 4463 (2009).

[39]S. Jain, D. Kumar, N. K. Swarnakar, and K. Thanki, Biomaterials **33**, 6758 (2012).

[40]M. L. Manca, D. Valenti, O. D. Sales, A. Nacher, A. M. Fadda, and M. Manconi, Int. J. Pharm. **472**, 102 (2014).

[41]K. Ren, L. Fourel, C. G. Rouvière, C. Albiges-Rizo, and C. Picart, Acta Biomater. **6**, 4238 (2010).

[42]D. Fischer, Y. Li, B. Ahlemeyer, J. Krieglstein, and T. Kissel, Biomaterials **24**, 1121 (2003).

[43]A. A. Yaroslavov, T. A. Sitnikova, A. A. Rakhnyanskaya, E. G. Yaroslavova, A. V. Sybachin, N. S. Melik-Nubarov, and G. B. Khomutov, Colloid Polym. Sci. **295**, 1405 (2017).

[44]A. J. Nolte, N. D. Treat, R. E. Cohen, and M. F. Rubner, Macromolecules **41**, 5793 (2008).

[45]G. Decher, Science **277**, 1232 (1997).

[46]M. C. Hsieh, R. J. Farris, and T. J. McCarthy, Macromolecules **30**, 8453 (1997).

[47]E. Donath, D. Walther, V. N. Shilov, E. Knippel, A. Budde, K. Lowack, C. A. Helm, and H. Möhwald, Langmuir **13**, 5294 (1997).

[48]F. Caruso, H. Lichtenfeld, E. Donath, and H. Möhwald, Macromolecules **32**, 2317 (1999).

[49]L. Liu, B. Ercan, L. Sun, K. S. Ziemer, and T. J. Webster, ACS Biomater. Sci. Eng. **2**, 122 (2016).

[50]B. G. Keselowsky, D. M. Collard, and A. J. García, J. Biomed. Mater. Res., A **66**, 247 (2003).

[51]K. Köhler, D. G. Shchukin, H. Möhwald, and G. B. Sukhorukov, J. Phys. Chem. B **109**, 18250 (2005).

[52]K. Köhler, H. Möhwald, and G. B. Sukhorukov, J. Phys. Chem. B **110**, 24002 (2006).

[53]C. Gao, S. Leporatti, S. Moya, E. Donath, and H. Möhwald, Chemistry **9**, 915 (2003).

[54]M. Zerball, A. Laschewsky, R. Köhler, and R. von Klitzing, Polymers **8**, 120 (2016).

[55]C. Lüdecke, M. Roth, W. Yu, U. Horn, J. Bossert, and K. D. Jandt, Colloids Surf., B **145**, 617 (2016).

[56]M. R. Park, M. K. Banks, B. Applegate, and T. J. Webster, Int. J. Nanomed **3**, 497 (2008).

[57]L. Bacakova, E. Filova, M. Parizek, T. Ruml, and V. Svorcik, Biotechnol. Adv. **29**, 739 (2011).

[58]C. J. Arias, R. L. Surmaitis, and J. B. Schlenoff, Langmuir **32**, 5412 (2016).